

Ferromagnetism in Mn-doped CuO

S. G. Yang,^{a)} T. Li, B. X. Gu, and Y. W. Du

National Laboratory of Solid State Microstructures, Nanjing University, Nanjing, China

H. Y. Sung, S. T. Hung, and C. Y. Wong

Materials Characterization and Preparation Facility, Hong Kong University of Science and Technology, Clear Water Bay, Kowloon, Hong Kong, China

A. B. Pakhomov^{b)}

Department of Materials Science and Engineering, University of Washington, Seattle, Washington 98195-2120

(Received 2 January 2003; accepted 12 September 2003)

Ferromagnetic properties have been observed in CuO doped with 3.5–15 at. % of Mn. The transition from ferromagnetic to paramagnetic phase at $T_C=80$ K is associated with the metal–insulator transition. Magnetoresistance is weakly negative in the vicinity of the transition, but positive in a wide range of temperatures below T_C . The experimental results suggest a possibility of interpretation in terms of the Zener double-exchange mechanism and strong electron–phonon interactions. © 2003 American Institute of Physics. [DOI: 10.1063/1.1623944]

Ferromagnetic semiconductors (FSs) are key materials for spin injection in electronic and optoelectronic semiconductor devices that can be controlled by weak magnetic field,¹ such as spin transistors, polarizing light-emitting diodes, and nonvolatile storage devices.^{2,3} As the efficiency of spin injection depends on the interface quality and impedance matching, all-semiconductor structures benefit the performance of spintronic devices.⁴ The best known FS structure realized experimentally is Mn-GaAs, with the highest Curie temperature of 110 K.⁵ In recent years, theoretical studies have been made on the origin of ferromagnetism (FM) in FSs, and room temperature (RT) FM predicted in semiconductors such as ZnO and AlN doped with magnetic ions.^{6–10} RT FM has been observed in diluted FM semiconductors Co-TiO₂, Mn-GaN, Cr-AlN, and Co-ZnO.^{11–15}

Pure CuO is an antiferromagnetic (AFM) semiconductor, which has been studied partly in relation to high-temperature cuprate superconductors.^{16–19} Susceptibility studies show three-dimensional AFM below 212 K.²⁰ Both doping with iron and other defects in CuO cause an increase of magnetic susceptibility, but FM has not been observed.²¹ In this letter, we report a realization of FM in CuO by Mn doping.

Five Mn-doped CuO samples were prepared by coprecipitation method using MnCl₂·4H₂O and CuCl₂·2H₂O as the starting materials, followed by annealing at 1000 °C for 10 h. Magnetic measurements were done on powders, while pellet-shaped samples, annealed together with the powder, were used for electric transport measurements. Mn and Cu concentrations in the Cu_{1-x}Mn_xO structures were determined by x-ray fluorescence. The Mn atomic fractions x of the five samples were 0.035, 0.066, 0.094, 0.127, and 0.150. No other elements were observed, except Mn, Cu, and O. Figure 1 shows the x-ray diffraction (XRD) results for sample Cu_{0.850}Mn_{0.150}O. The samples consist of the main phase CuO (*C2/c*) and a small amount of CuMn₂O₄. The

presence of CuMn₂O₄ increases with increasing Mn concentration.

Magnetic properties of the Mn-CuO samples were studied on a superconducting quantum interference device (Quantum Design MPMS-5S). All samples show magnetic hysteresis at $T<80$ K, with coercive fields of 110, 590, 500, 70, and 260 Oe for $x=0.035, 0.066, 0.094, 0.127$ and 0.150 , respectively, at 5 K. The spontaneous magnetic moment per Mn atom is estimated to be up to $\sim 1.5 \mu_B$. Figure 2 shows hysteresis loops for the samples with $x=0.066, 0.094$, and 0.15 at $T=5$ K. Temperature dependence of magnetization at 10 Oe was measured in the range from 5 to 120 K, both in zero-field-cooled (ZFC) and field-cooled (FC) conditions. Figure 3 shows the results for sample Cu_{0.850}Mn_{0.150}O, showing two phase transitions, one at about $T_N=30$ K, and another at $T_C=80$ K. These transitions were also observed in other samples at the same temperatures. The inset of Fig. 3 shows temperature dependence of inverse susceptibility, indicating that the sample is paramagnetic above $T_C=80$ K.

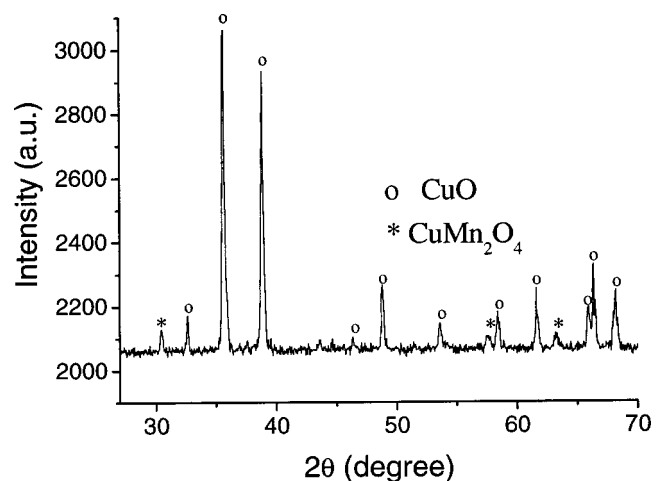


FIG. 1. XRD pattern of the sample Cu_{0.850}Mn_{0.150}O.

^{a)}Electronic mail: sgyang@nju.edu.cn

^{b)}Electronic mail: pakhomov@u.washington.edu

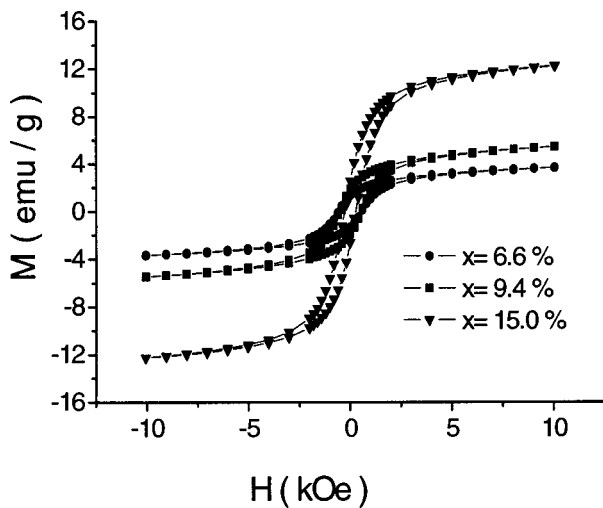


FIG. 2. Magnetic hysteresis loops for the samples $\text{Cu}_{1-x}\text{Mn}_x\text{O}$ with $x=0.066, 0.094,$ and 0.150 .

The positive Weiss constant ($\theta_p \approx 80$ K) suggests that this transition is between paramagnetic and FM phases.

Figure 4 shows the temperature dependence of resistivity of the sample $\text{Cu}_{0.850}\text{Mn}_{0.150}\text{O}$, both in zero field (open symbols) and in an applied field of $H=30$ kOe. There is a critical point at 80 K. Above $T_C=80$ K, resistance decreases with increasing temperature, following a relation $\rho = \rho_0 \exp[(T_0/T)^{1/2}]$ (see upper inset of Fig. 4), which indicates variable range hopping modified by the Coulomb gap at the Fermi level.²² Below 80 K, the behavior is “metallic”-like; however, notice that the value of resistivity remains very high at $\sim 10^4 \Omega \text{ cm}$. This result is different from that of pure CuO, where resistivity decreases monotonically with increasing temperature.¹⁸ We observe no sizeable shift in the critical temperature in applied field. Magnetoresistance (MR) is weakly negative in the vicinity of T_C , and positive at $T < T_C$. Resistivity of the samples increases dramatically with decreasing the Mn concentration x . The low inset of Fig. 4 shows that the sample with $x=0.127$ is about 50 times more resistive than at $x=0.150$. Resistance of samples with lower x near T_C was above the limitations of our measurement setup.

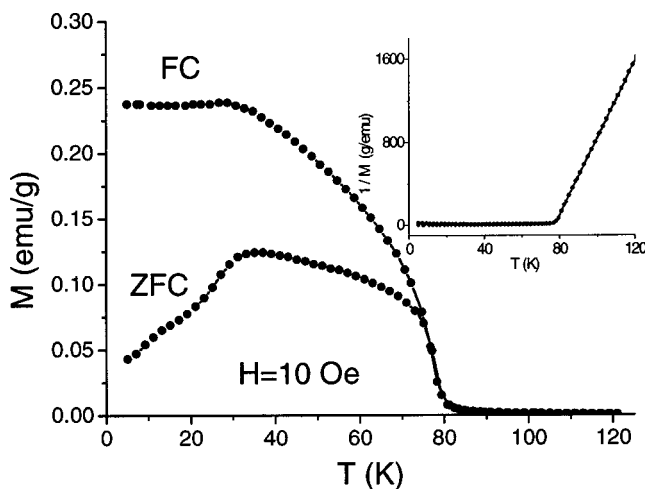


FIG. 3. ZFC and FC magnetization of the sample $\text{Cu}_{0.850}\text{Mn}_{0.150}\text{O}$ at $H=10$ Oe. The inset shows inverse magnetization as a function of temperature.

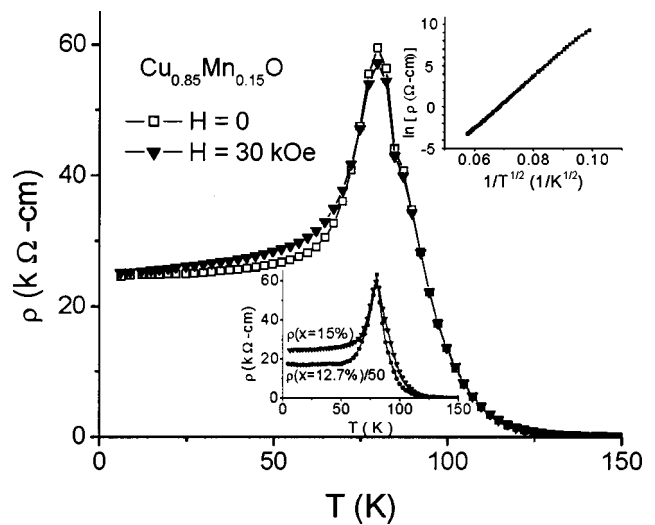


FIG. 4. Resistivity as a function of temperature for sample $\text{Cu}_{0.850}\text{Mn}_{0.150}\text{O}$ in the external fields $H=0$ and $H=30$ kOe. Upper inset: logarithm of resistivity vs $1/T^{1/2}$ for $T > 100$ K. Lower inset: comparison of resistivities of samples with 15% Mn and 12.7% Mn doping. The latter is scaled down by a factor of about 50.

In order to determine the magnetic contribution from the CuMn_2O_4 phase, we prepared a standard pure CuMn_2O_4 sample at the same conditions. Pure phase was confirmed by XRD. Figure 5 shows the magnetization curve of the CuMn_2O_4 sample measured at $T=4.3$ K. Temperature dependence of magnetization for this standard sample is shown in the inset of the Fig. 5. This material shows canted AFM behavior with the Néel temperature of about $T_N \approx 30$ K. Hence we can attribute the anomaly at 30 K seen in Fig. 3 to the presence of small amounts (less than 10% based on XRD analyses) of CuMn_2O_4 phase. This phase does not contribute to the observed hysteresis (Fig. 2). FM with the Curie temperature of $T_C=80$ K is thus attributed to the Mn-CuO phase.

The crystal structure of CuO is monoclinic ($C2/c$), in which Cu atoms are coordinated to four coplanar oxygen atoms situated at the corners of an almost rectangular parallelogram. With two more distant apical O atoms, a distorted octahedron is formed because of large Jahn–Teller effect. The cell parameters for a natural crystal of tenorite are $a=4.662$ Å, $b=3.417$ Å, $c=5.118$ Å, and $\beta=97^\circ 29'$. There

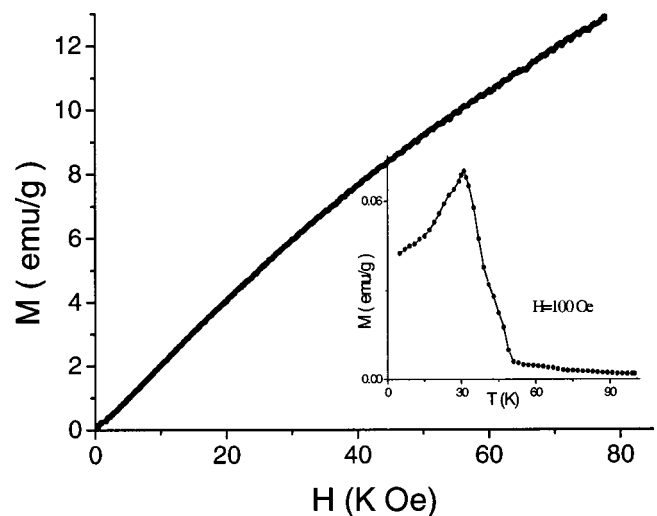


FIG. 5. Field dependence of magnetization of standard CuMn_2O_4 sample at $T=4.3$ K. Inset is the moment as a function of temperature at $H=100$ Oe.

are two bond angles of Cu–O–Cu: 146° and 99° . Magnetic measurements and neutron diffraction experiments have shown that the structure is AFM, with a commensurate propagation vector $(1/2, 0, -1/2)$ below the Néel temperature.²³

Depending on the valence (2, 3, or 4), a Mn ion has up to five *d*-electrons with the total spin of $S=5/2$, 2, or $3/2$, respectively, due to Hund's rule. A Cu ion has a total spin of $1/2$, hence Mn ions doped in CuO have extra moments. Although the extra moments should be coupled to the lattice of Cu spins via superexchange, random dilute doping will not provide a net spontaneous magnetization. Correlation of magnetic properties with conduction allows us to assume that a carrier-mediated mechanism is involved in FM ordering. The Zener double-exchange mechanism has been successfully applied both to diluted magnetic semiconductors such as Mn-GaAs⁸ and the colossal MR (CMR) perovskites $\text{Re}_{1-x}\text{A}_x\text{MnO}_3$, where Re is a rare-earth element and A is a divalent alkali element.²⁴ It may be also valid in our Mn-CuO structures. Extending the analogy, we suggest that a fraction of *d*-electron states can be available for hopping between Mn sites and mediating FM through the Hund's rule coupling. We notice in this relation that conductivity increases dramatically with Mn doping, and no additional doping is needed for FM; however, crystal defects may play some role in creation of holes. It has been shown²⁴ that explanation of the resistive anomaly at T_C requires in addition a strong electron–phonon interaction. Such interaction is also likely in the Mn-doped CuO structure, and leads to localization of magnetic polarons at $T > T_C$.

Along with certain similarities with the CMR behavior, we notice considerable differences, such as relative insensitivity of the transition temperature to external field, very high resistivity in the “metallic” nonactivational regime, and positive MR at $T < T_C$. These differences can be partly explained by the large average hopping distances between Mn sites in diluted Mn-CuO, which increases the resistivity and leads to positive MR via shrinkage of the wave functions (decreasing localization length) in external field.²² Correlations with AFM host may modify the mechanism and contribute to the differences with the known materials.

In conclusion, ferromagnetism has been observed in Mn-doped CuO with a Curie temperature $T_C=80$ K. The transition is associated with resistive anomaly. Magnetoresistance at $T < T_C$ is positive. Interpretation is given in terms of the Zener model and strong electron–phonon interactions. Possible effects of the antiferromagnetic host require more theoretical studies.

This work was supported by the Hong Kong SAR Government Innovation and Technology Commission, Project AF/155/99, “973 project,” and the National Natural Science Foundation. One of the authors (A.B.P.) acknowledges partial support at the University of Washington by the Campbell Endowment.

- ¹H. Ohno, D. Chiba, F. Matsukura, T. Omlia, E. Abe, T. Dietl, Y. Ohno, and K. Ohtani, *Nature (London)* **408**, 944 (2000).
- ²R. Fiederling, M. Keim, G. Reuscher, W. Ossau, G. Schmidt, A. Waag, and L. W. Molenkamp, *Nature (London)* **402**, 787 (1999).
- ³Y. Ohno, D. K. Young, B. Beschoten, F. Matsukura, H. Ohno, and D. D. Awschalom, *Nature (London)* **402**, 790 (1999).
- ⁴M. Oestreich, J. Hubner, D. Hagele, D. J. Klar, W. Heimbrodt, W. W. Ruhle, D. E. Ashenford, and B. Lunn, *Appl. Phys. Lett.* **74**, 1251 (1999).
- ⁵F. Matsukura, H. Ohno, A. Shen, and Y. Sugawara, *Phys. Rev. B* **57**, R2037 (1998).
- ⁶H. Akai, *Phys. Rev. Lett.* **81**, 3002 (1998).
- ⁷J. König, H. H. Lin, and A. H. MacDonald, *Phys. Rev. Lett.* **84**, 5628 (2000).
- ⁸T. Dietl, H. Ohno, F. Matsukura, J. Cibert, and D. Ferrand, *Science* **287**, 1019 (2000).
- ⁹V. I. Litvinov and V. K. Dugaev, *Phys. Rev. Lett.* **86**, 5593 (2001).
- ¹⁰J. Schliemann and A. H. MacDonald, *Phys. Rev. Lett.* **88**, 137201 (2002).
- ¹¹Y. Matsumoto, M. Murakami, T. Shono *et al.*, *Science* **291**, 854 (2001).
- ¹²S. A. Chambers, S. Thevuthasan, R. F. C. Farrow, R. F. Marks, J. U. Thiele, L. Folks, M. G. Samant, A. J. Kellock, N. Ruzycki, D. L. Ederer, and U. Diebold, *Appl. Phys. Lett.* **79**, 3467 (2001).
- ¹³N. Theodoropoulou, A. F. Hebard, M. E. Overberg, C. R. Abernathy, S. J. Pearton, S. N. G. Chu, and R. G. Wilson, *Appl. Phys. Lett.* **78**, 3475 (2001).
- ¹⁴S. G. Yang, A. B. Pakhomov, S. T. Hung, and C. Y. Wong, *Appl. Phys. Lett.* **81**, 2418 (2002); S. Y. Wu, H. X. Liu, L. Gu, R. K. Singh, L. Budd, M. van Schilfgaarde, M. R. McCartney, D. V. Smith, and N. Newman, *ibid.* **82**, 3047 (2003).
- ¹⁵K. Ueda, H. Tabata, and T. Kawai, *Appl. Phys. Lett.* **79**, 988 (2001); S. G. Yang, A. B. Pakhomov, S. T. Hung, and C. Y. Wong, *IEEE Trans. Magn.* **38**, 2877 (2002).
- ¹⁶J. W. Loram, K. A. Mirza, C. P. Joyce, and A. J. Osborne, *Europhys. Lett.* **8**, 263 (1989).
- ¹⁷A. Junod, D. Eckert, G. Triscone, J. Muller, and W. Reichardt, *J. Phys.: Condens. Matter* **1**, 8021 (1989).
- ¹⁸X. G. Zheng, C. N. Xu, E. Tanaka, Y. Tomokiyo, M. Suzuki, and E. S. Otabe, *Physica C* **357–360**, 181 (2001).
- ¹⁹M. Sohma, K. Kawaguchi, and Y. Fujii, *J. Appl. Phys.* **77**, 1189 (1995).
- ²⁰T. I. Arbutova, A. A. Samokhvalou, I. B. Smolyak, B. V. Karpenko, N. M. Chebotov, and S. V. Naumov, *J. Magn. Magn. Mater.* **95**, 168 (1991).
- ²¹R. A. Borzi, S. J. Stewart, G. Punte, R. C. Mercader, G. A. Curatchet, R. D. Zysler, and M. Tovar, *J. Appl. Phys.* **87**, 4870 (2000).
- ²²B. I. Shklovskii and A. L. Efros, *Electronic Properties of Doped Semiconductors* (Springer, Berlin, New York, 1984).
- ²³J. B. Forsyth, P. J. Brown, and B. M. Wanklyn, *J. Phys. C* **21**, 2917 (1988).
- ²⁴A. J. Millis, B. I. Shraiman, and R. Mueller, *Appl. Phys. Lett.* **77**, 175 (1996); A. J. Millis, *Nature (London)* **392**, 147 (1998).